

Impact of Imperfect Channel Estimation on the Performance of Amplify-and-Forward Relaying

Berna Gedik and Murat Uysal

Abstract—In this paper, we investigate the error rate performance of amplify-and-forward (AF) relaying with imperfect channel estimation. We consider a single-relay scenario with orthogonal and non-orthogonal AF (OAF and NAF) cooperative protocols. Two pilot-symbol-assisted receiver architectures are studied: In the mismatched-coherent receiver, the complex fading channel coefficients (i.e., both phase and amplitude) are estimated based on a linear minimum-mean-squared-error estimation approach and fed to a coherent sub-optimal maximum likelihood decoder as if the channels were perfectly known. In the partially-coherent receiver, channel amplitude is ignored and phase is estimated by a phase locked loop. For both receiver types, we analyze the achievable diversity orders for cooperative protocols under consideration and quantify the impact of channel estimation through the derivation of pairwise error probability. Our performance analysis reveals that a second order diversity order is obtained for the considered single-relay scenario indicating that full diversity is extracted. Our simulation results demonstrate that the performance degradation due to channel estimation with respect to the genie bound (i.e., perfect channel state information) is as small as 1.1dB based on the employed detector. Performance results further show that partially-coherent receiver presents a similar performance to mismatched-receiver for sufficiently large loop SNRs although channel amplitude is completely ignored.

Index Terms—Transmission technology, cooperative diversity, space-time coding.

I. INTRODUCTION

COOPERATIVE diversity has been proposed as a powerful means to enhance the performance of high-rate communications over wireless fading channels [1]–[3]. It realizes spatial diversity advantages in a distributed manner where two or more nodes (each with single antenna) share their antennas to mimic a virtual antenna array. Cooperative diversity has garnered much attention in the past few years with a flurry of papers (see e.g., the survey papers [4]–[6] and the references therein) providing insights into capacity and power savings realizable through cooperation. However, most of the research efforts on this topic have been mainly limited to some idealistic assumptions such as the availability of perfect channel state information (CSI). Some research efforts on differential and non-coherent detection should be noted [7]–[11] in a related context. Under the assumption of coherent detection, the fading channel coefficients need to be first

estimated and then used in the detection process. In decode-and-forward (DF) relaying, both relay and destination require a reliable channel estimate. In amplify-and-forward (AF) relaying, knowledge of CSI is required at the destination terminal and may be required at the relay as well depending on the adopted scaling factor [12]. The quality of channel estimates inevitably affects the overall performance of relay-assisted transmission and might become a performance limiting factor. Channel estimation problem in the context of DF relaying basically consists of individual estimation of source-to-relay and relay-to-destination channels. On the other hand, in AF relaying, a cascaded channel from source-to-destination needs to be estimated. Although it can be possibly argued that this could be disintegrated into individual channel estimations (i.e., separate estimations of source-to-relay and relay-to-destination channels) through the injection of a “clean” pilot symbol at relay, such an approach would require additional pilot symbols, therefore reduce the bandwidth and power efficiency. It would also require the forward-feedback of source-to-relay channel estimate from the relay to destination terminal which would be subject to further distortions during transmission. Therefore, in this paper, we devote our attention to AF relaying with channel estimation of the overall cascaded channel.

To the best of our knowledge, coherent detection with imperfect channel estimation for AF relaying has been first addressed by Mheidat and Uysal in [13] and independently by Patel and Stuber in [14], [15]. The main focus in [13] and its journal version [11] is actually the derivation of a non-coherent detector based on a maximum likelihood sequence estimator for distributed space-time block codes whereas the performance of a mismatched-coherent receiver (i.e., coherent detection with imperfect channel estimation) is studied as a benchmark. On the other hand, [15] considers a multi-hop relay scenario, derives a channel estimator tailored for cascaded Rayleigh fading channel, and further presents an approximate bit error rate performance analysis for a mismatched-coherent receiver. Furthermore, in [37], Quek *et al.* propose power allocation algorithms for coherent and non-coherent AF relay networks taking into account imperfect channel knowledge.

In this paper, we investigate the effects of channel estimation on the performance of both orthogonal AF (OAF) [16] and non-orthogonal AF (NAF) relaying¹ [17] which correspond to distributed SIMO (single-input multiple-output) and MIMO (multiple-input multiple-output) implementations, respectively [3]. We consider mismatched-coherent and partially-coherent receivers at the destination terminal. In mismatched-coherent

Manuscript received February 22, 2008; revised June 21, 2008; accepted August 19, 2008. The associate editor coordinating the review of this paper and approving it for publication was D. Dardari.

M. Uysal is with the Department of Electrical and Computer Engineering, University of Waterloo, Canada. B. Gedik is currently affiliated with General Electric Company (e-mail: {bgedik, muysal}@engmail.uwaterloo.ca).

The work of M. Uysal is supported in part by an NSERC Special Opportunity Grant (SROPJ305821-05).

Digital Object Identifier 10.1109/TWC.2008.080252

¹Orthogonal and non-orthogonal AaF relaying are referred as Protocol II and Protocol I, respectively in [3].

receiver, the channel coefficients are first estimated through pilot symbols based on a linear minimum-mean-squared-error estimation (LMMSE) approach and then fed to a coherent maximum likelihood (ML) decoder as if the channel was perfectly known. In partially-coherent receiver, the estimates of channel phase information are obtained through a phase lock loop (PLL) while no effort is made for the estimation of channel amplitudes. Considering these two receiver-types, we quantify the impact of channel estimation on OAF and NAF relaying through the derivations of pairwise error probability (PEP) and a comprehensive Monte-Carlo simulation study.

The rest of the paper is organized as follows: In Section II, we introduce the relay-assisted transmission and describe the received signal models for OAF and NAF relaying. In Section III, we describe pilot-symbol-assisted LMMSE channel estimation and PLL-aided phase estimation. In Section IV, we provide PEP expressions for the two receiver types under consideration. In Section V, we discuss the effect of relay location on channel estimation. In Section VI, we present an extensive Monte-Carlo simulation study to demonstrate the error rate performance of OAF and NAF cooperation protocols with mismatched-coherent and partially-coherent receivers. The conclusions are given in Section VII. Finally, the details of PEP derivations are provided in the appendixes.

Notation: $(\cdot)^T, (\cdot)^*, (\cdot)^H$ denote transpose, conjugate, and Hermitian transpose operations, respectively. $E(\cdot)$ denotes expectation. $|\cdot|$ denotes the absolute value, $\|\cdot\|$ denotes the Frobenius norm and \mathbf{I}_N denotes the identity matrix of size N . $\text{var}(\cdot)$ denotes the variance of a random variable. $\det(\cdot)$, $\text{diag}(\cdot)$, and $\text{trace}(\cdot)$ denote the determinant, diagonal, and trace of a matrix, respectively. i denotes $\sqrt{-1}$. $\text{Re}(\cdot)$ denotes real part. Bold upper-case letters denote the matrices and bold lower-case letters denote the vectors.

II. SYSTEM MODEL

We consider a single-relay scenario where each of the half-duplex nodes is equipped with a single pair of transmit and receive antennas (Fig. 1). To incorporate the effect of relay geometry in our model, we consider a channel model which takes into account both long-term free-space path loss and short-term Rayleigh fading. The path loss is proportional to d^{-a} where d is the propagation distance and a is the path loss coefficient. In Fig. 1, d_{SD} , d_{SR} , and d_{RD} denote the distances of source-to-destination (S→D), source-to-relay (S→R), and relay-to-destination (R→D) links, respectively, and θ is the angle between lines S→R and R→D. Assuming the path loss in S→D to be unity, the relative gain of S→R and R→D links are defined as $G_{SR} = (d_{SD}/d_{SR})^a$ and $G_{RD} = (d_{SD}/d_{RD})^a$ [18].

We consider two cooperation protocols: In OAF protocol [16], the source terminal communicates with the relay and destination terminals over the first signaling interval. In the second signaling interval, only the relay terminal communicates with the destination terminal. NAF protocol [3], [17] differs from OAF version in the sense that the source continues transmission over the second interval. It is apparent that signal conveyed to the relay and destination terminals over the two time slots is same for OAF relaying whereas NAF protocol can

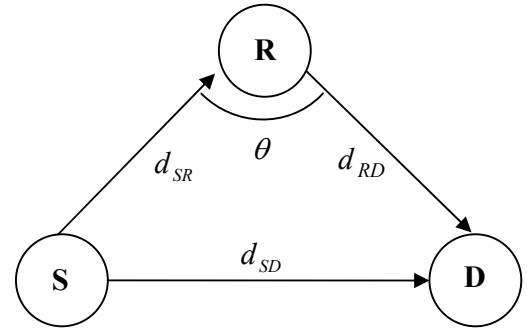


Fig. 1. Relay-assisted transmission model

potentially convey different signals to the relay and destination terminals. This makes possible the deployment of various conventional space-time codes (originally proposed for co-located antennas) in a distributed scenario².

A. NAF protocol

Although any conventional space-time code can, in principle, be used in conjunction with NAF protocol, we consider Golden code of [19], which has been recently shown to achieve optimum diversity-multiplexing tradeoff in the single relay AF case [20]. Let $\mathbf{x} = [x_1 \ x_2 \ x_3 \ x_4]^T$ denote M-PSK (phase shift keying) modulation signals with normalized energy, i.e., $E[|x_i|^2] = 1$. Before transmission, the modulation signals are fed into a precoder given by [19]

$$\mathbf{P} = \begin{bmatrix} \alpha & \alpha\Theta & 0 & 0 \\ 0 & 0 & i\bar{\alpha} & i\bar{\alpha}\bar{\Theta} \\ 0 & 0 & \alpha & \alpha\Theta \\ \bar{\alpha} & \bar{\alpha}\bar{\Theta} & 0 & 0 \end{bmatrix} \quad (1)$$

where $\Theta = (1 + \sqrt{5})/2$, $\bar{\Theta} = (1 - \sqrt{5})/2$, $\alpha = (1 + i - i\Theta)/\sqrt{5}$, $\bar{\alpha} = (1 + i - i\bar{\Theta})/\sqrt{5}$. The output of the precoder is given by $\mathbf{c} = \mathbf{P}\mathbf{x} = [c_1 \ c_2 \ c_3 \ c_4]^T$ where $c_1 = \alpha(x_1 + \Theta x_2)$, $c_2 = i\bar{\alpha}(x_3 + \bar{\Theta}x_4)$, $c_3 = \alpha(x_3 + \Theta x_4)$, and $c_4 = \bar{\alpha}(x_1 + \bar{\Theta}x_2)$. In the first signaling interval, the codeword c_1 is transmitted from the source with energy E . Considering path-loss effects, the received signals at the relay and destination are given as

$$r_{R1} = \sqrt{G_{SR}E}h_{SR}c_1 + n_{R1}, \quad (2)$$

$$r_{D1} = \sqrt{E}h_{SD}c_1 + n_{D1}. \quad (3)$$

The relay terminal normalizes the received signal by a factor of $\sqrt{E[|r_{R1}|^2]}$ to have average unit energy and then re-transmits the normalized signal within the second time slot. The source terminal simultaneously transmits the codeword

²It should be noted that the use of space-time block codes (STBC) has been proposed by Laneman et.al. in [2] for OAF protocol. Their proposed use of STBC, however, implements coding across the relay nodes assuming a scenario with more than one relay and differs from the distributed STBC setup in [3] proposed for NAF protocol which involves the source terminal in a single-relay scenario.

c_2 . Therefore, the destination receives a superposition of the signals transmitted by the relay and source transmission as

$$r_{D2} = \sqrt{G_{RD} \frac{E}{2}} h_{RD} \frac{r_{R1}}{\sqrt{E[|r_{R1}|^2]}} + \sqrt{\frac{E}{2}} h_{SD} c_2 + n \quad (4)$$

where scaling by $1/\sqrt{2}$ is included to ensure the total power consumption limited by E in a particular time slot. In (2)-(4), h_{SR} , h_{SD} , and h_{RD} denote fading coefficients over S→R, S→D, and R→D links respectively, and are modeled as zero-mean complex Gaussian random variables with variance of 0.5 per dimension leading to a Rayleigh fading channel model. n_R , n_{D1} , and n are the independent samples of zero-mean complex Gaussian random variables with variance $N_0/2$ per dimension, which model the additive noise terms. Replacing $\sqrt{E[|r_{R1}|^2]} = \sqrt{G_{SR}E\kappa + N_0}$ with $\kappa = |\alpha|^2(1 + \Theta^2)$ in (4), we obtain

$$r_{D2} = \sqrt{\frac{0.5G_{SR}G_{RD}E^2}{G_{SR}E\kappa + N_0}} h_{SR}h_{RD}c_1 + \sqrt{0.5E} h_{SD}c_2 + \tilde{n}_1 \quad (5)$$

where $\tilde{n}_1 = \sqrt{0.5G_{RD}E/(G_{SR}E\kappa + N_0)} h_{RD}n_{R1} + n$. Due to the term involving $h_{RD}n_{R1}$, \tilde{n}_1 is of Gaussian nature which makes the analysis intractable. However, as in [15], [21], we can treat it as Gaussian noise with the same average power. Therefore, \tilde{n}_1 is assumed to be complex Gaussian with statistics $\tilde{n}_1 \sim CN(0, N_0(1 + 0.5G_{RD}E\sigma_{h_{RD}}^2/(G_{SR}E\kappa + N_0)))$. The destination terminal normalizes r_{D2} by a factor of $\sqrt{1 + (0.5G_{RD}E)\sigma_{h_{RD}}^2/(G_{SR}E\kappa + N_0)}$ yielding

$$r_{D2} = \sqrt{A_1 E} h_{SR}h_{RD}c_1 + \sqrt{A_2 E} h_{SD}c_2 + n_{D2} \quad (6)$$

where n_{D2} is zero mean complex Gaussian random variable with a variance of N_0 . In (6), A_1 and A_2 are defined as

$$A_1 = \frac{0.5G_{SR}G_{RD}E/N_0}{1 + G_{SR}E/N_0 + 0.5\sigma_{h_{RD}}^2 G_{RD}E/N_0}, \quad (7)$$

$$A_2 = \frac{0.5(1 + G_{SR}E/N_0)}{1 + G_{SR}E/N_0 + 0.5\sigma_{h_{RD}}^2 G_{RD}E/N_0}. \quad (8)$$

The codewords c_3 and c_4 are transmitted from the source in the third and fourth time slots, respectively. The corresponding received signal models are obtained, similar to (3) and (6), as

$$r_{D3} = \sqrt{E} h_{SD}c_3 + n_{D3}, \quad (9)$$

$$r_{D4} = \sqrt{A_1 E} h_{SR}h_{RD}c_3 + \sqrt{A_2 E} h_{SD}c_4 + n_{D4}. \quad (10)$$

Defining $\mathbf{r} = [r_{D1} \ r_{D2} \ r_{D3} \ r_{D4}]^T$, $\mathbf{n} = [n_{D1} \ n_{D2} \ n_{D3} \ n_{D4}]^T$, and $\mathbf{h} = [h_{SR}h_{RD} \ h_{SD}]^T = [h_{SRD} \ h_{SD}]^T$, the received signals over four time slots can be rewritten in a compact matrix form as $\mathbf{r} = \mathbf{X}_D \mathbf{h} + \mathbf{n}$ where \mathbf{X}_D is given by

$$\mathbf{X}_D = \begin{bmatrix} 0 & \sqrt{A_1 E} c_1 & 0 & \sqrt{A_1 E} c_3 \\ \sqrt{E} c_1 & \sqrt{A_2 E} c_2 & \sqrt{E} c_3 & \sqrt{A_2 E} c_4 \end{bmatrix}^T. \quad (11)$$

B. OAF protocol

This protocol is a distributed SIMO structure and implements receive diversity in a distributed fashion. Let x be the M-PSK signal transmitted from the source in the first time slot. The received signals at relay and destination are given by

$$r_R = \sqrt{G_{SR}E} h_{SR}x + n_R, \quad (12)$$

$$r_{D1} = \sqrt{E} h_{SD}x + n_{D1}. \quad (13)$$

The relay terminal normalizes the received signal by a factor of $\sqrt{E[|r_R|^2]} = \sqrt{G_{SR}E + N_0}$ to have average unit energy and then re-transmits the normalized signal within the second time slot. The received signal model at the destination in the second time is given by

$$r_{D2} = \sqrt{\frac{G_{SR}G_{RD}E^2}{G_{SR}E + N_0}} h_{SR}h_{RD}x + \tilde{n}_1 \quad (14)$$

where $\tilde{n}_1 = \sqrt{G_{RD}E/(G_{SR}E + N_0)} h_{RD}n_R + n$. The destination terminal normalizes r_{D2} by a factor of $\sqrt{1 + G_{RD}E\sigma_{h_{RD}}^2/(G_{SR}E + N_0)}$ resulting in

$$r_{D2} = \sqrt{B_1 E} h_{SR}h_{RD}x + n_{D2} \quad (15)$$

where B_1 is defined as

$$B_1 = \frac{G_{SR}G_{RD}E/N_0}{1 + G_{SR}E/N_0 + \sigma_{h_{RD}}^2 G_{RD}E/N_0}. \quad (16)$$

Defining $\mathbf{r} = [r_{D1} \ r_{D2}]^T$ and $\mathbf{n} = [n_{D1} \ n_{D2}]^T$, the received signals can be rewritten in a matrix form as $\mathbf{r} = \mathbf{X}_D \mathbf{h} + \mathbf{n}$ where \mathbf{X}_D is given by

$$\mathbf{X}_D = \begin{bmatrix} 0 & \sqrt{E} \\ \sqrt{B_1 E} & 0 \end{bmatrix} x. \quad (17)$$

III. MISMATCHED-COHERENT AND PARTIALLY-COHERENT RECEIVERS

In this section, we consider two different pilot-symbol-assisted receiver architectures: In the first receiver, the complex fading channel coefficients (i.e., both phase and amplitude) are estimated based on an LMMSE approach and fed to a coherent ML decoder. This results in so-called mismatched receiver [22]. In the second receiver, channel amplitude is ignored. Only phase information of the channels is estimated by a PLL and these estimates are used in a partially-coherent receiver [23]. We assume perfect synchronization throughout the paper.

Let \mathbf{X}_{lT} , $l = 1, 2, \dots, N$, and \mathbf{X}_{jD} , $j = 1, 2, \dots, M$ denote the pilot and data matrices transmitted by the source terminal at transmission blocks l and j . Here, N and M denote the number of training and data transmission blocks, respectively. The length of data transmission block is equal to the codeword length which is 2 and 4 for OAF and NAF protocols, c.f., (11) and (17). The received signal is therefore given by

$$\mathbf{X}_{Tot} = \left[\underbrace{\mathbf{X}_{1T} \cdots \mathbf{X}_{NT}}_{\mathbf{X}_T} \ \underbrace{\mathbf{X}_{1D} \cdots \mathbf{X}_{MD}}_{\mathbf{X}_D} \right]^T. \quad (18)$$

A. Mismatched-coherent detection with LMMSE estimator

The LMMSE estimate of the channel matrix can be obtained as $\hat{\mathbf{h}} = \mathbf{B}\mathbf{r}_T$ where $\mathbf{r}_T = \mathbf{X}_T\mathbf{h} + \mathbf{n}_T$ is the received signal during the training period and \mathbf{B} is a matrix obtained through the minimization of $E[\|\mathbf{B}\mathbf{r}_T - \mathbf{h}\|^2]$. This minimization yields [24]

$$\mathbf{B} = E\left(\mathbf{h}\mathbf{r}_T^H\right) E\left(\mathbf{r}_T\mathbf{r}_T^H\right)^{-1}. \quad (19)$$

Using $E\left(\mathbf{h}\mathbf{h}^H\right) = \mathbf{I}_2$, the channel estimate $\hat{\mathbf{h}} = \mathbf{h} - \mathbf{e}$ is obtained as

$$\hat{\mathbf{h}} = \begin{bmatrix} \hat{h}_{SRD} & \hat{h}_{SD} \end{bmatrix}^T = \mathbf{X}_T^H (\mathbf{X}_T \mathbf{X}_T^H + N_0 \mathbf{I}_2)^{-1} \mathbf{r}_T. \quad (20)$$

The covariance matrix of estimation errors $\mathbf{e} = \begin{bmatrix} e_{SRD} & e_{SD} \end{bmatrix}^T$ is given by

$$\begin{aligned} \mathbf{C}_e &= E\left(\mathbf{h}\mathbf{h}^H\right) - \mathbf{B}E\left(\mathbf{r}_T\mathbf{r}_T^H\right)\mathbf{B}^H \\ &= N_0\left(\mathbf{X}_T^H\mathbf{X}_T + N_0\mathbf{I}_2\right)^{-1}. \end{aligned} \quad (21)$$

The channel estimate $\hat{\mathbf{h}}$ is then used to minimize the following sub-optimal ML metric ³

$$\arg \min_{\mathfrak{N}} \left\| \mathbf{r} - \mathbf{X}_D \hat{\mathbf{h}} \right\|^2 \quad (22)$$

where $\mathfrak{N} = \{x_1, x_2, x_3, x_4\}$ for NAF protocol and $\mathfrak{N} = \{x\}$ for OAF protocol. The exhaustive search required in (22) can be avoided by using low complexity sphere decoding techniques [34], [35].

B. Partially-coherent detection with PLL estimator

Let $h_{SRD} = |h_{SRD}|e^{j\varphi_{SRD}}$ and $h_{SD} = |h_{SD}|e^{j\varphi_{SD}}$ be the polar coordinates representations of the complex fading coefficients. φ_{SRD} and φ_{SD} are the phases introduced by S→R→D and S→D channels. We assume a first order PLL at the destination terminal. Upon receiving the signal \mathbf{r}_T during the training phase, PLL first compares the phases of the input signal and the locally generated oscillator output, then generates a control signal that is a function of the phase difference which is minimized to produce phase estimates $\hat{\varphi}_{SD}$ and $\hat{\varphi}_{SRD}$. The estimation errors are denoted as $\varepsilon_{SRD} = \varphi_{SRD} - \hat{\varphi}_{SRD}$ and $\varepsilon_{SD} = \varphi_{SD} - \hat{\varphi}_{SD}$ for S→R→D and S→D links, respectively. Their distribution can be well approximated by Tikhonov probability density function [25]

$$p_\varepsilon(\varepsilon) = \frac{\exp(\rho \cos \varepsilon)}{2\pi I_0(\rho)}, \quad -\pi \leq \varepsilon \leq \pi \quad (23)$$

where we drop the index S→R→D and S→D for notational convenience. Here, $I_0(\cdot)$ is the zeroth order modified Bessel function of the first kind [26] and ρ is the loop signal-to-noise ratio defined as [25]

$$\rho = \frac{\xi}{B_L T} \quad (24)$$

where T denotes the symbol duration, B_L is the loop bandwidth, and ξ is the instantaneous received signal-to-noise-ratio

³The optimal ML metric can be obtained by maximizing the probability density function $p(\mathbf{r}, \mathbf{r}_T | \mathbf{X}_D, \mathbf{X}_T)$ [22]. This optimal metric makes use of the received pilot symbols for the detection of transmitted data and would include some terms to reflect the covariance of the effective noise. However, its form is complicated and restricts its practical feasibility.

[33]. If PLL is assumed to be in lock position, ε is sufficiently small; therefore, phase errors can be approximated as zero mean Gaussian random variables with variance $\sigma_\varepsilon^2 = 1/\rho$. These phase estimates are used in partially-coherent detection to minimize the metric

$$\arg \min_{\mathfrak{N}} \left\| \mathbf{r} - \mathbf{X}_D \hat{\varphi} \right\|^2 \quad (25)$$

where $\hat{\varphi} = \begin{bmatrix} e^{j\hat{\varphi}_{SRD}} & e^{j\hat{\varphi}_{SD}} \end{bmatrix}^T$ and channel amplitudes are taken equal to one [23].

IV. DIVERSITY GAIN ANALYSIS

In this section, we investigate the achievable diversity order for the cooperative schemes under consideration through the derivation of PEP. PEP is the building block for the derivation of union bounds to the error probability. It is widely used in the literature to predict the attainable diversity order where the closed-form error probability expressions are unavailable. Let $P(\mathbf{X}_D \rightarrow \hat{\mathbf{X}}_D)$ denote PEP where the transmitted codeword vector and the erroneously-decoded codeword matrices are given by \mathbf{X}_D and $\hat{\mathbf{X}}_D$, respectively. Following the derivation steps in Appendix A, PEP for NAF relaying with Golden code and mismatched-coherent receiver can be given as

$$\begin{aligned} P(\mathbf{X}_D \rightarrow \hat{\mathbf{X}}_D) &< \frac{4SNR_{eff}^{-2} / (\lambda_{\min}^2 \kappa_1 \kappa_2)}{(1 - \sigma_{eSD}^2)(1 - \sigma_{eSR}^2)(1 - \sigma_{eRD}^2)} \\ &\times \exp\left(\frac{2SNR_{eff}^{-1} / (\lambda_{\min} \kappa_2)}{(1 - \sigma_{eSR}^2)(1 - \sigma_{eRD}^2)}\right) \\ &\times \Gamma\left(0, \frac{2SNR_{eff}^{-1} / (\lambda_{\min} \kappa_2)}{(1 - \sigma_{eSR}^2)(1 - \sigma_{eRD}^2)}\right) \end{aligned} \quad (26)$$

where $SNR_{eff} = E/2\Lambda$. Here, Λ is trace of the covariance matrix for effective noise which contains both additive Gaussian channel noise and channel estimation error and is given by (50) of Appendix A. In (26), κ_1, κ_2 are defined by $\kappa_1 = \kappa + A_2\kappa'$ and $\kappa_2 = A_1\kappa$ where $\kappa = |\alpha|^2(1 + \Theta^2)$ and $\kappa' = |\bar{\alpha}|^2(1 + \bar{\Theta}^2)$. λ_{\min} denotes the minimum value of $\lambda_1 + \lambda_3$ and $\lambda_2 + \lambda_4$ where $\lambda_1, \lambda_2, \lambda_3,$ and λ_4 are the eigenvalues of $(\mathbf{x} - \hat{\mathbf{x}})(\mathbf{x} - \hat{\mathbf{x}})^H$. $\sigma_{eSD}^2, \sigma_{eSR}^2,$ and σ_{eRD}^2 denote variances of S→D, S→R, and R→D channel estimation errors and are, respectively, given by

$$\sigma_{eSD}^2 = (E/N_0)^{-1} / \left(N(2\kappa + \kappa') + (E/N_0)^{-1} \right), \quad (27)$$

$$\sigma_{eSR}^2 = (E/N_0)^{-1} / \left(2NG_{SR}\kappa + (E/N_0)^{-1} \right), \quad (28)$$

$$\sigma_{eRD}^2 = (E/N_0)^{-1} / \left(NG_{RD}\kappa + (E/N_0)^{-1} \right). \quad (29)$$

For large SNR_{eff} values, exponential term in (26) goes to zero and we can use the approximation $\lim_{t \rightarrow 0} \Gamma(0, t) \approx -\log(t)$

for the gamma term [28]. Then, $P(\mathbf{X}_D \rightarrow \hat{\mathbf{X}}_D)$ reduces to

$$\begin{aligned} P(\mathbf{X}_D \rightarrow \hat{\mathbf{X}}_D) &< \frac{4SNR_{eff}^{-2}}{\lambda_{\min}^2 \kappa_1 \kappa_2 (1 - \sigma_{eSD}^2)(1 - \sigma_{eSR}^2)(1 - \sigma_{eRD}^2)} \\ &\times \log\left(\frac{SNR_{eff} \lambda_{\min} \kappa_2 (1 - \sigma_{eSR}^2)(1 - \sigma_{eRD}^2)}{2}\right) \end{aligned} \quad (30)$$

Under high SNR_{eff} assumption, $\log(SNR_{eff})$ term can be ignored with respect to the dominating term SNR_{eff}^{-2} . Thus, asymptotically, second order diversity is achieved, extracting the full diversity for the considered scenario with single relay. We observe that the presence of channel estimation errors does not affect the diversity order. The PEP expression for the perfect CSI case can be simply obtained when the estimation error variances become zero. Let $P_{genie}(\mathbf{X}_D \rightarrow \hat{\mathbf{X}}_D)$ denote the PEP for perfect CSI, then the performance degradation due to channel estimation is given by

$$\begin{aligned} \Xi &= \frac{P(\mathbf{X}_D \rightarrow \hat{\mathbf{X}}_D)}{P_{genie}(\mathbf{X}_D \rightarrow \hat{\mathbf{X}}_D)} \\ &= \frac{(\Lambda/N_0)^2}{(1-\sigma_{e_{SD}}^2)(1-\sigma_{e_{SR}}^2)(1-\sigma_{e_{RD}}^2)} \\ &\quad \times \log \left(\frac{E\lambda_{min}\kappa_2}{4} \left[\frac{(1-\sigma_{e_{SR}}^2)(1-\sigma_{e_{RD}}^2)}{\Lambda} - \frac{1}{N_0} \right] \right). \end{aligned} \quad (31)$$

By increasing pilot symbol power, estimation error variances approach zero (i.e., $\sigma_{e_{SR}}^2, \sigma_{e_{SD}}^2 \rightarrow 0$) leading to $\log \Xi = \log 1 = 0$.

PEP for OAF relaying with mismatched coherent receiver is given as (see Appendix B for details of the derivation)

$$\begin{aligned} P(\mathbf{X}_D \rightarrow \hat{\mathbf{X}}_D) &\leq \frac{4SNR_{eff}^{-2}/(\lambda^2 B_1)}{(1-\sigma_{e_{SD}}^2)(1-\sigma_{e_{SR}}^2)(1-\sigma_{e_{RD}}^2)} \\ &\quad \times \exp \left(\frac{2SNR_{eff}^{-1}/(\lambda B_1)}{(1-\sigma_{e_{SR}}^2)(1-\sigma_{e_{RD}}^2)} \right) \\ &\quad \times \Gamma \left(0, \frac{2SNR_{eff}^{-1}/(\lambda B_1)}{(1-\sigma_{e_{SR}}^2)(1-\sigma_{e_{RD}}^2)} \right) \end{aligned} \quad (32)$$

where $\lambda = |x - \hat{x}|^2$ and $SNR_{eff} = E/2\Lambda$. Λ contains both channel estimation error and additive noise variances and is given by (63) of Appendix B. In (32), $\sigma_{e_{SD}}^2$, $\sigma_{e_{SR}}^2$, and $\sigma_{e_{RD}}^2$ denote variances of S→D, S→R, and R→D channel estimation errors and are, respectively, given by

$$\sigma_{e_{SD}}^2 = (E/N_0)^{-1}/(N + (E/N_0)^{-1}), \quad (33)$$

$$\sigma_{e_{SR}}^2 = (E/N_0)^{-1}/(NG_{SR} + (E/N_0)^{-1}), \quad (34)$$

$$\sigma_{e_{RD}}^2 = (E/N_0)^{-1}/(NG_{RD} + (E/N_0)^{-1}). \quad (35)$$

For large SNR_{eff} values, (32) reduces to

$$\begin{aligned} P(\mathbf{X}_D \rightarrow \hat{\mathbf{X}}_D) &\leq \frac{4SNR_{eff}^{-2}/(\lambda^2 B_1)}{(1-\sigma_{e_{SD}}^2)(1-\sigma_{e_{SR}}^2)(1-\sigma_{e_{RD}}^2)} \\ &\quad \times \log \left(\frac{SNR_{eff}\lambda B_1(1-\sigma_{e_{SR}}^2)(1-\sigma_{e_{RD}}^2)}{2} \right) \end{aligned} \quad (36)$$

$$\begin{aligned} \Xi &= \frac{(\Lambda/N_0)^2}{(1-\sigma_{e_{SD}}^2)(1-\sigma_{e_{SR}}^2)(1-\sigma_{e_{RD}}^2)} \\ &\quad \times \log \left(\frac{E\lambda B_1}{4} \left[\frac{(1-\sigma_{e_{SR}}^2)(1-\sigma_{e_{RD}}^2)}{\Lambda} - \frac{1}{N_0} \right] \right) \end{aligned} \quad (37)$$

As $\sigma_{e_{SR}}^2, \sigma_{e_{SD}}^2 \rightarrow 0$, (36) reduces to perfect CSI case reported in [29] and $\log \Xi$ becomes 0.

Finally, for OAF relaying with partially-coherent receiver, we obtain the PEP as, (see Appendix C for details of the derivation)

$$\begin{aligned} P(\mathbf{X}_D \rightarrow \hat{\mathbf{X}}_D) &< \frac{SNR_{eff}^{-2} \sqrt{(\Delta_2 B_L T / (2\Delta_1 + 2B_1 \Delta_1))^2}}{B_1^2 \Delta_1^2} \sqrt{\frac{(\Delta_2 B_L T / (2\Delta_1 + 2B_1 \Delta_1))^2}{\Delta_1^2 + SNR_{eff}^{-1}}} \\ &\quad \times \exp \left(\frac{\Delta_2 B_L T}{2} + \frac{SNR_{eff}^{-1}}{B_1^2 \Delta_1^2} \right) \Gamma \left(0, \frac{SNR_{eff}^{-1}}{B_1^2 \Delta_1^2} \right) \\ &\quad \times K_1 \left(\sqrt{\left(\frac{\Delta_2 B_L T}{2 + 2B_1} \right)^2 + \frac{(\Delta_2 B_L T / (2 + 2B_1))^2 SNR_{eff}^{-1}}{\Delta_1^2}} \right) \end{aligned} \quad (38)$$

where $SNR_{eff} = E/[2N_0(1 - \cos(\theta_\Delta))(1 + B_1)]$, $\Delta_1 = (1 - \cos(\theta_\Delta))$, $\Delta_2 = (1 - \cos(\theta_\Delta) - 2 \sin(\theta_\Delta))$, and $\cos(\theta_\Delta) = Re\{x\hat{x}^*\}$. For large values of SNR_{eff} , we use the approximation $K_v(z) \approx 0.5\Gamma(v)(2/z)^v$, $z < 1$ [28] reducing (38) to

$$\begin{aligned} P(\mathbf{X}_D \rightarrow \hat{\mathbf{X}}_D) &< \frac{SNR_{eff}^{-2}}{B_1^2 \Delta_1^4} \exp \left(\frac{\Delta_2 B_L T}{2} \right) \\ &\quad \times \log(SNR_{eff} B_1^2 \Delta_1^2) \end{aligned} \quad (39)$$

indicating a second order diversity. Performance degradation with respect to partially-coherent receiver having perfect channel phase knowledge is given by

$$\Xi = \exp \left(\frac{\Delta_2 B_L T}{2} \right). \quad (40)$$

As the loop signal-to-noise ratio (which is inversely proportional to $B_L T$) increases, estimation of the channel phases in PLL become error free and therefore the term in (40) approaches one.

V. EFFECT OF RELAY LOCATION ON THE QUALITY OF CHANNEL ESTIMATES

In this section, we investigate the effect of relay location on the quality of channel estimates. Let Σ_{SRD} denote mean squared error (MSE) of S→R→D channel estimate. To minimize MSE with respect to relay location, we need to solve the following constrained optimization problem

$$\begin{aligned} &\text{minimize } \Sigma_{SRD} \\ &G_{SR}, G_{RD} \end{aligned} \quad (41)$$

s.t. $G_{SR}^{-2/a} + G_{RD}^{-2/a} - 2G_{SR}^{-1/a}G_{RD}^{-1/a}\cos\theta = 1$ where the constraint equation is obtained through law of cosines between relative gains G_{SR} and G_{RD} considering the relay geometry (c.f., Fig. 1). For Golden coded pilot symbols p_{1i} and p_{3i} , replacing $\mathbf{X}_T = [\sqrt{A_1 E} p_{11} \quad \sqrt{A_1 E} p_{31} \quad \dots \quad \sqrt{A_1 E} p_{1N} \quad \sqrt{A_1 E} p_{3N}]^T$ in $N_0(\mathbf{X}_T^H \mathbf{X}_T + N_0)^{-1}$, we can obtain Σ_{SRD} of NAF protocol as

$$\Sigma_{SRD} = \frac{(E/N_0)^{-1}}{2A_1 N \kappa + (E/N_0)^{-1}} \quad (42)$$

where A_1 is a function of G_{SR} and G_{RD} , c.f. (7). Assume a scenario with path loss coefficient $a = 2$ and $\theta = \pi$. Then, we have $G_{RD} = (1 + 1/\sqrt{\eta})^2$ and $G_{SR} = \eta(1 + 1/\sqrt{\eta})^2$ with

$\eta = G_{SR}/G_{RD}$. Taking the derivative of (42) with respect to η and equating to zero, we have

$$\frac{\partial \Sigma_{SRD}}{\partial \eta} = \frac{(EN\kappa/N_0)^2 v^3 (-2/\sqrt{\eta} + v/\eta + v\chi_1/m_1)/(\eta m_1)}{((EN\kappa/N_0)^2 v^4 / (\eta m_1) + 1)^2} = 0 \quad (43)$$

where $v = \sqrt{\eta} + 1$, $m_1 = 1 + v^2 E(\kappa + 1/2\eta)/N_0$, and $\chi_1 = vE(\kappa + 1/2\eta - v/2\eta\sqrt{\eta})/(\sqrt{\eta}N_0)$. The numeric solutions of (43) for various E/N_0 are provided in Table I.

TABLE I
RELAY LOCATIONS THAT MINIMIZE MSE ($N = 1$)

$\eta = G_{SR}/G_{RD}$ [dB]	$\theta = \pi$	$\theta = 3\pi/4$	$\theta = 2\pi/3$
$E/N_0 = 10$ dB	-6.210 dB	-7.55 dB	-9.32 dB
$E/N_0 = 25$ dB	-6.021 dB	-7.20 dB	-8.74 dB
$E/N_0 = 35$ dB	-6.021 dB	-7.19 dB	-8.73 dB
$E/N_0 = 100$ dB	-6.020 dB	-7.19 dB	-8.73 dB

Note that Σ_{SRD} is a convex function of relay location η (see Fig. 3). Therefore, the results in Table I are, in fact, global minimums of the optimization problem. We observe from the table that relay location which minimizes MSE remains nearly constant for a wide range of SNR values. Negative values of $\eta = G_{SR}/G_{RD}$ (in dB) indicate that quality of channel estimation improves when relay is closer to the destination. Similar observations can be made for other values of θ presented in Table I. As θ decreases, optimum relay location comes even closer to destination.

For OAF protocol, replacing $\mathbf{X}_T = [\sqrt{B_1 E} p_1 \dots \sqrt{B_1 E} p_N]^T$ in $N_0(\mathbf{X}_T^H \mathbf{X}_T + N_0)^{-1}$, Σ_{SRD} can be obtained as

$$\Sigma_{SRD} = \frac{(E/N_0)^{-1}}{B_1 N + (E/N_0)^{-1}} \quad (44)$$

where B_1 is a function of G_{SR} and G_{RD} , c.f. (16). Taking the derivative of (44) with respect to $\eta = G_{SR}/G_{RD}$, we have

$$\frac{\partial \Sigma_{SRD}}{\partial \eta} = \frac{(E/N_0)^2 v^3 (-2/\sqrt{\eta} + v/\eta + v\chi_2/m_2)/(\eta m_2)}{((E/N_0)^2 v^4 / (\eta m_2) + 1)^2} = 0 \quad (45)$$

where $m_2 = 1 + v^2 E(1 + 1/\eta)/N_0$ and $\chi_2 = vE(1 + 1/\eta - v/\eta\sqrt{\eta})/(\sqrt{\eta}N_0)$. Solving (45), we have $\eta = 0$ dB independent of E/N_0 value. Hence, minimum MSE is obtained when relay is in the mid-point between source and destination.

VI. SIMULATION RESULTS AND DISCUSSION

In this section, we present an extensive Monte-Carlo simulation study to demonstrate the performance of OAF and NAF relaying with mismatched-coherent and partially-coherent receivers. In our simulations, we consider NAF protocol with Golden code assuming 4-PSK modulation. This code achieves a throughput of 4 bits/sec/Hz in a non-cooperative 2x2 MIMO system and a throughput of 2 bits/sec/Hz in a single-relay cooperative communication system [19], [20]. To make a fair comparison, we consider OAF relaying and non-cooperative direct transmission with 16-PSK and 4-PSK, respectively.

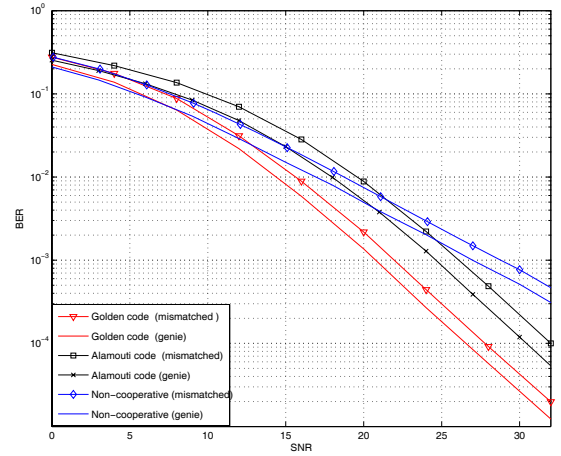


Fig. 2. BER performance of Golden-coded and Alamouti-coded NAF protocol with mismatched-coherent and genie receivers ($G_{SR}/G_{RD} = 0$).

In Fig. 2, we present the bit error rate (BER) performance of Golden-coded NAF protocol with a mismatched-coherent receiver for a scenario in which the relay is located in the midway of source-to-destination link, i.e., $G_{SR}/G_{RD} = 0$ dB. We assume $a = 2$ and $\theta = \pi$. The performance of genie-aided receiver (i.e., perfect CSI), non-cooperative direct transmission (i.e., no relaying), and NAF protocol with Alamouti code are further included as benchmarks. Assuming 16-PSK modulation, Alamouti code achieves a throughput of 4 bits/sec/Hz in non-cooperative 2x1 MIMO system and a throughput of 2 bits/sec/Hz in single-relay cooperative communication system. It is observed that Golden-coded NAF protocol with both perfect and imperfect channel estimation yields a diversity order of two confirming our PEP analysis. The mismatched-coherent detection results in a performance loss of approximately 1.5 dB at $\text{BER} = 5.10^{-3}$ with respect to the genie bound. Although Alamouti-coded NAF protocol extracts a diversity order of two as well, it is significantly outperformed by its Golden-coded counterpart. Specifically, at $\text{BER} = 5.10^{-3}$, we observe a performance difference of 4 dB between two codes. Our results further demonstrate that Golden code has a slightly better robustness than Alamouti in the presence of imperfect channel estimation.

In Fig. 3, we demonstrate MSE and BER performance of NAF protocol as a function of relay location at SNR values of 10dB and 28dB. From Fig. 3.a and 3.b, we observe that the relay location which minimizes the estimation error is independent of SNR value and takes place approximately at $G_{SR}/G_{RD} = -6$ dB. This confirms our earlier analytical derivations in Section V (c.f. Table I). For low SNR values (e.g., SNR=10dB), we observe from Fig. 3.c that error rate performance of Golden code improves slightly as relay continues to move away from the destination. However for high SNRs, a better error rate performance is obtained when the relay is close to the destination (i.e., farther than -6 dB location). For such large negative values, relay is close to the destination and in such a scenario, cooperative scheme mimics the behavior of a receive diversity scheme with two

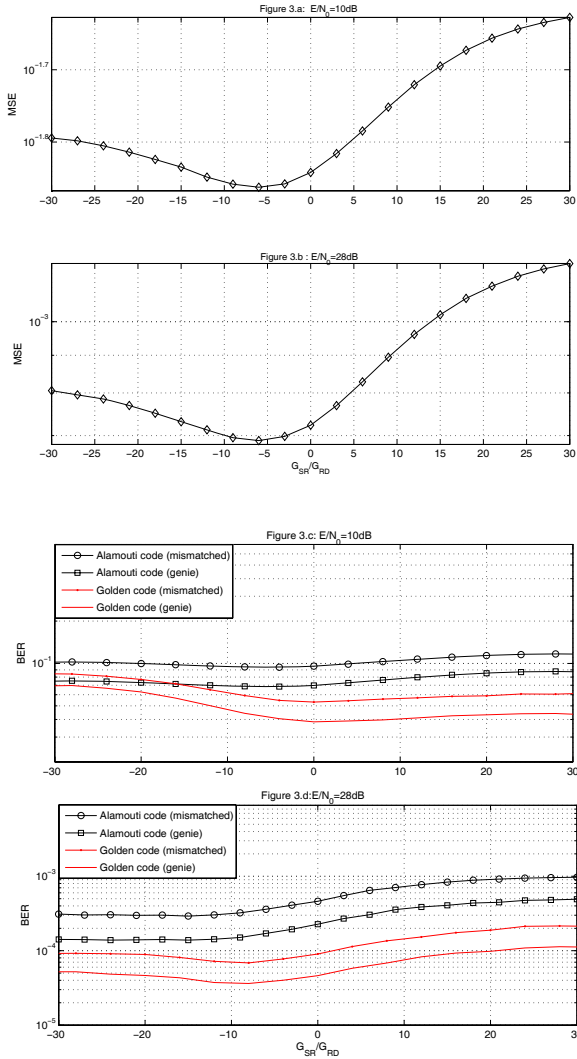


Fig. 3. MSE and BER performance of NAF protocol with respect to relay location $E/N_0 = 10$ and 28dB.

co-located antennas. This demonstrates that nature of the cooperation protocol dominates the BER performance rather than the channel estimation quality.

In Fig. 4, we present BER performance of OAF relaying with mismatched-coherent and partially-coherent receivers for $G_{SR}/G_{RD} = 0\text{dB}$ along with the genie bound. For partially-coherent detection with PLL-aided phase estimation, we consider two different B_{LT} values. For $B_{LT} = 0.03$ and 0.3, performance degradations with respect to genie bound are, respectively, 1.1 dB and 4dB at $\text{BER} = 5 \cdot 10^{-3}$. This is an expected result as large B_{LT} values result in inefficient phase estimation; whereas for small B_{LT} values the estimation error variance tends to zero. It is interesting to note that partially-coherent detector with $B_{LT} = 0.03$ is able to slightly outperform the mismatched-coherent receiver although no effort is made for channel amplitude estimation. This points out that a reliable channel phase information is more essential in the detection process than the channel amplitude. Further comparison of Figs. 2 and 4 reveal that NAF protocol with Alamouti code provides an identical performance to that of OAF protocol. This observation has been earlier reported in [29] for perfect CSI case. Since Golden-coded NAF has a

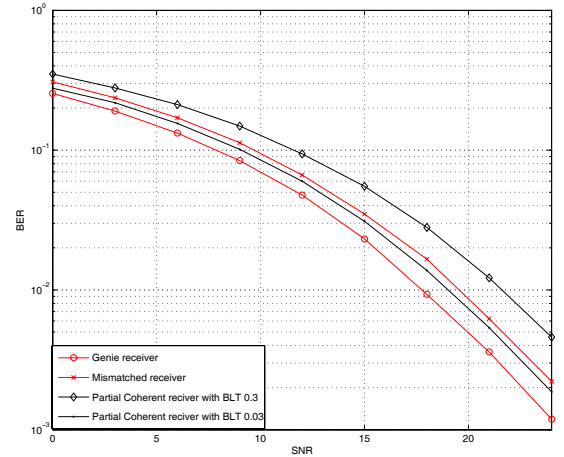


Fig. 4. BER performance of OAF protocol with mismatched-coherent and partially-coherent receivers ($G_{SR}/G_{RD} = 0$).

much superior performance over both OAF and Alamouti-coded NAF, it becomes the obvious choice for distributed implementation.

In Fig. 5, we provide MSE and BER performance of OAF relaying as a function of relay location. Both mismatched-coherent and partially-coherent receivers are considered. We observe from Fig. 5.a and Fig. 5.b that OAF protocol experiences the minimum estimation error when the relay is in the mid-point confirming our derivations in Section V. Our results in Fig. 5.c and Fig. 5.d demonstrate that error rate performance improves as relay moves closer to the destination. This is similar to our earlier observations for Fig. 3. Specifically, for $G_{SR}/G_{RD} = -30\text{dB}$ and $\text{SNR} = 28\text{dB}$, the performance degradations with respect to genie bound are, respectively, 1.5×10^{-4} , 1.6×10^{-4} , 5.6×10^{-4} dB for mismatched-coherent receiver, partially-coherent receivers with $B_{LT} = 0.03$ and $B_{LT} = 0.3$. For $G_{SR}/G_{RD} = 30\text{dB}$, the performance degradations are 4.2×10^{-4} , 1.2×10^{-4} and 5.4×10^{-4} respectively.

In Fig. 6, we illustrate BER performance of OAF relaying with mismatched-coherent receiver as a function of number of pilot symbols N . It is observed that BER improves as the number of pilot symbols increase. As the performance degradation caused by estimation errors becomes sufficiently small, a saturation point is reached where further increase in pilot symbol number will not result in a significant change, but rather reduce the data throughput [30].

VII. CONCLUSION

In this paper, we have investigated the impact of channel estimation on the performance of amplify-and-forward relaying considering mismatched-coherent and partially-coherent receivers at the destination terminal. Our performance analysis, through the derivation of PEP expressions, reveals that a second-order diversity order is obtained for the single-relay scenario in all considered combinations of protocols and receiver types. It has been observed that Golden-coded NAF

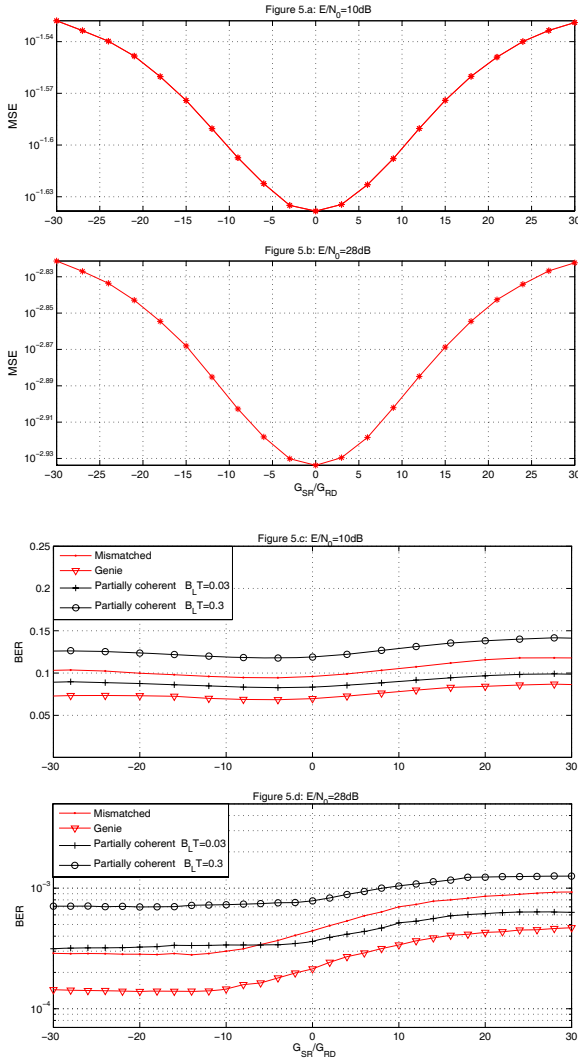


Fig. 5. MSE and BER performance of OAF protocol with respect to relay location ($E/N_0 = 10$ and 28 dB).

protocol is always superior to OAF protocol and Alamouti-coded NAF protocol even if the channel knowledge at the receiver is imperfect. Specifically, it is observed that Golden-coded NAF protocol with a mismatched-coherent receiver operates within 1.5 dB (at a target of $\text{BER} = 5 \cdot 10^{-3}$) of the genie bound and outperforms Alamouti-coded NAF scheme by 4dB. Performance results of OAF protocol reveal that partially-coherent detection has performance degradation as small as 1.1 dB for sufficiently large loop SNRs and can even outperform mismatched-receiver although the channel amplitudes are completely ignored.

We have also investigated relay locations which minimize MSE of the channel estimates. These locations are determined as $G_{SR}/G_{RD} = 0$ dB (i.e., when relay is midway between source and destination) for OAF protocol and $G_{SR}/G_{RD} = -6$ dB for Golden-coded NAF protocol (i.e., when relay is closer to destination). Our simulation results further reveal that these locations do have a minimal impact on BER performance as error rate performance is mainly governed by the location of relay imposed by nature of the protocols. Specifically, error rate performance gets better when relay

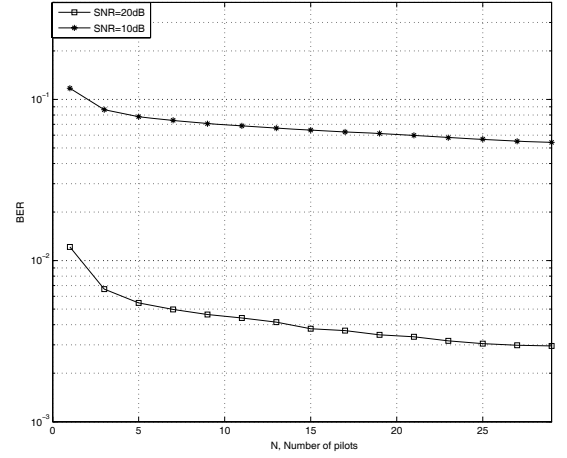


Fig. 6. BER performance of OAF protocol with respect to number of pilots.

moves close to the destination for both protocols which, for very large negative values of G_{SR}/G_{RD} , mimic a virtual receive diversity scheme.

APPENDIX A

In this appendix, we present the derivation of PEP for Golden coded NAF protocol with mismatched-coherent detector. Replacing the channel estimate $\hat{\mathbf{h}} = \mathbf{h} - \mathbf{e}$ in the received signal vector $\mathbf{r} = \mathbf{X}_D \mathbf{h} + \mathbf{n}$, we have $\mathbf{r} = \mathbf{X}_D \hat{\mathbf{h}} + \bar{\mathbf{n}}$ where we define the effective noise term $\bar{\mathbf{n}} = \mathbf{X}_D \mathbf{e} + \mathbf{n}$. Under the assumption of Gaussian channel estimation errors, an upper PEP bound for transmitted codeword matrix \mathbf{X}_D and erroneously decoded codeword matrix $\hat{\mathbf{X}}_D$ is given by ⁴ [11], [36]

$$P(\mathbf{X}_D \rightarrow \hat{\mathbf{X}}_D | \hat{\mathbf{h}}) \leq \exp\left(-\frac{\|(\mathbf{X}_D - \hat{\mathbf{X}}_D)\hat{\mathbf{h}}\|^2}{4\text{trace}\{\mathbf{E}(\bar{\mathbf{n}}\bar{\mathbf{n}}^H)\}}\right) \quad (46)$$

where \mathbf{X}_D is defined earlier by (11). For simplifying the ensuing derivation, we rewrite $\mathbf{r} = \mathbf{X}_D \hat{\mathbf{h}} + \mathbf{X}_D \mathbf{e} + \mathbf{n}$ as $\mathbf{r} = \hat{\mathbf{H}}\mathbf{x} + \bar{\mathbf{n}}$ where $\bar{\mathbf{n}} = \delta\mathbf{x} + \mathbf{n}$. $\hat{\mathbf{H}}$ and δ are, respectively, given by (47) and (48) (both can be found at the top of the next page). Replacing (47) and (48) in (46), we have

$$P(\mathbf{x} \rightarrow \hat{\mathbf{x}} | \hat{\mathbf{H}}) \leq \exp\left(-\frac{\|\hat{\mathbf{H}}(\mathbf{x} - \hat{\mathbf{x}})\|^2}{4\Lambda}\right) = \exp\left(-\frac{1}{4\Lambda}\text{trace}\{\hat{\mathbf{H}}\mathbf{A}\hat{\mathbf{H}}^H\}\right) \quad (49)$$

where we define $\mathbf{A} = (\mathbf{x} - \hat{\mathbf{x}})(\mathbf{x} - \hat{\mathbf{x}})^H$ and

$$\Lambda = \text{trace}\{\mathbf{E}(\bar{\mathbf{n}}\bar{\mathbf{n}}^H)\} = 4N_0 + 2\sigma_{e_{SD}}^2 \kappa_1 E + 2\sigma_{e_{SRD}}^2 \kappa_2 E. \quad (50)$$

Here, $\sigma_{e_{SD}}^2$ and $\sigma_{e_{SRD}}^2$ denote the variances of $S \rightarrow D$ and $S \rightarrow R \rightarrow D$ link estimation errors, and are given by

$$\sigma_{e_{SD}}^2 = (E/N_0)^{-1} / \left(N(2\kappa + \kappa') + (E/N_0)^{-1}\right), \quad (51)$$

⁴Note that the components of the effective noise term $\bar{\mathbf{n}}$ do not have identical variance. To simplify the analysis, we replace them with independent virtual noise components with their variance given as $\text{trace}\{\mathbf{E}(\bar{\mathbf{n}}\bar{\mathbf{n}}^H)\} = \sum_{k=1}^4 \text{var}(\bar{n}_k)$.

$$\hat{\mathbf{H}} = \begin{bmatrix} \alpha\sqrt{E}\hat{h}_{SD} & \alpha\Theta\sqrt{E}\hat{h}_{SD} & 0 & 0 \\ \alpha\sqrt{A_1E}\hat{h}_{SRD} & \alpha\Theta\sqrt{A_1E}\hat{h}_{SRD} & i\bar{\alpha}\sqrt{A_2E}\hat{h}_{SD} & i\bar{\alpha}\Theta\sqrt{A_2E}\hat{h}_{SD} \\ 0 & 0 & \alpha\sqrt{E}\hat{h}_{SD} & \alpha\Theta\sqrt{E}\hat{h}_{SD} \\ \bar{\alpha}\sqrt{A_2E}\hat{h}_{SD} & \bar{\alpha}\Theta\sqrt{A_2E}\hat{h}_{SD} & \alpha\sqrt{A_1E}\hat{h}_{SRD} & \alpha\Theta\sqrt{A_1E}\hat{h}_{SRD} \end{bmatrix} \quad (47)$$

$$\delta = \begin{bmatrix} \alpha\sqrt{E}e_{SD} & \alpha\Theta\sqrt{E}e_{SD} & 0 & 0 \\ \alpha\sqrt{A_1E}e_{SRD} & \alpha\Theta\sqrt{A_1E}e_{SRD} & i\bar{\alpha}\sqrt{A_2E}e_{SD} & i\bar{\alpha}\Theta\sqrt{A_2E}e_{SD} \\ 0 & 0 & \alpha\sqrt{E}e_{SD} & \alpha\Theta\sqrt{E}e_{SD} \\ \bar{\alpha}\sqrt{A_2E}e_{SD} & \bar{\alpha}\Theta\sqrt{A_2E}e_{SD} & \alpha\sqrt{A_1E}e_{SRD} & \alpha\Theta\sqrt{A_1E}e_{SRD} \end{bmatrix} \quad (48)$$

$$\sigma_{e_{SRD}}^2 = (E/N_0)^{-1} / \left(2N\kappa_2 + (E/N_0)^{-1} \right). \quad (52)$$

Since \mathbf{A} in (49) is Hermitian and non-negative definite, it can be decomposed into $\mathbf{A} = \mathbf{U}\mathbf{D}\mathbf{U}^H$ where \mathbf{U} is unitary matrix and $\mathbf{D} = \text{diag}\{\lambda_1, \lambda_2, \lambda_3, \lambda_4\}$ is a diagonal matrix having real-valued eigenvalues of \mathbf{A} . Replacing \mathbf{A} with $\mathbf{U}\mathbf{D}\mathbf{U}^H$, (49) becomes

$$P(\mathbf{x} \rightarrow \hat{\mathbf{x}} | \hat{\mathbf{H}}) \leq \exp \left(-\frac{1}{4\Lambda} \text{trace} \left\{ \underbrace{\hat{\mathbf{H}}\mathbf{U}\mathbf{D}}_{\hat{\mathbf{H}}'} \underbrace{\mathbf{U}^H\hat{\mathbf{H}}}_{\hat{\mathbf{H}}'^H} \right\} \right).$$

Noting that multiplication by a unitary matrix does not change the statistics of $\hat{\mathbf{H}}$, we get (53) (which can be found at the next page) where $\bar{\lambda}_1 = \lambda_1 + \lambda_3$ and $\bar{\lambda}_2 = \lambda_2 + \lambda_4$. Defining $\lambda_{\min} = \min\{\bar{\lambda}_1, \bar{\lambda}_2\}$, the unconditional PEP can be found as

$$P(\mathbf{x} \rightarrow \hat{\mathbf{x}}) < \Psi_{|\hat{h}_{SD}|^2} \left(-\frac{E\kappa_1\lambda_{\min}}{4\Lambda} \right) \times \Psi_{|\hat{h}_{SRD}|^2} \left(-\frac{E\kappa_2\lambda_{\min}}{4\Lambda} \right) \quad (54)$$

where $\Psi_{|\hat{h}_{SD}|^2}$ and $\Psi_{|\hat{h}_{SRD}|^2}$ are the moment generating functions (MGFs) of $|\hat{h}_{SD}|^2$ and $|\hat{h}_{SRD}|^2$ respectively. $|\hat{h}_{SD}|^2$ is central chi-squared distributed with second degree of freedom. Hence its MGF can be readily found as [23]

$$\Psi_{|\hat{h}_{SD}|^2}(-s) = 1 / \left(1 + s\sigma_{\hat{h}_{SD}}^2 \right) \quad (55)$$

where the variance of S \rightarrow D channel estimate is $\sigma_{\hat{h}_{SD}}^2 = 1 - \sigma_{e_{SD}}^2$. For the S \rightarrow R \rightarrow D channel, \hat{h}_{SRD} is the estimate of the product of two Gaussian terms, i.e., $h_{SRD} = h_{SR}h_{RD}$. Unfortunately, the exact distribution function of \hat{h}_{SRD} is unknown. Here, we follow a similar approach to [15] where the estimate of cascaded channels is modeled as the product of estimates of individual channels: Assume S \rightarrow R and R \rightarrow D channels are estimated individually as $h_{SR} = \hat{h}_{SR} + e_{SR}$ and $h_{RD} = \hat{h}_{RD} + e_{RD}$ where the estimation errors are modeled as zero-mean complex Gaussian random variables with variances given as

$$\sigma_{e_{SR}}^2 = (E/N_0)^{-1} / \left(2NG_{SR}\kappa + (E/N_0)^{-1} \right), \quad (56)$$

$$\sigma_{e_{RD}}^2 = (E/N_0)^{-1} / \left(NG_{RD}\kappa + (E/N_0)^{-1} \right). \quad (57)$$

The variance of $\hat{h}_{SR}\hat{h}_{RD}$ (i.e., the product of individual estimates) is then found as

$$\begin{aligned} \text{var}(\hat{h}_{SR}\hat{h}_{RD}) &= (1 - \sigma_{e_{SR}}^2) (1 - \sigma_{e_{RD}}^2) \\ &= 1 - \sigma_{e_{SR}}^2 - \sigma_{e_{RD}}^2 + \sigma_{e_{SR}}^2 \sigma_{e_{RD}}^2. \end{aligned} \quad (58)$$

On the other hand, the variance of \hat{h}_{SRD} (i.e., estimate of the cascaded channel) is given by

$$\text{var}(\hat{h}_{SRD}) = 1 - \sigma_{e_{SRD}}^2 = 2N\kappa_2 / \left(2N\kappa_2 + (E/N_0)^{-1} \right).$$

Asymptotic relative efficiency of two estimates is defined as [27]

$$\frac{\text{var}(\hat{h}_{SR}\hat{h}_{RD})}{\text{var}(\hat{h}_{SRD})} = \frac{1 - \sigma_{e_{SR}}^2 - \sigma_{e_{RD}}^2 + \sigma_{e_{SR}}^2 \sigma_{e_{RD}}^2}{1 - \sigma_{e_{SRD}}^2}. \quad (59)$$

For high SNR and sufficiently large pilot numbers, the relative efficiencies of two estimators become the same, i.e.,

$$\lim_{\substack{E/N_0 \rightarrow \infty \\ N \rightarrow \infty}} \frac{\text{var}(\hat{h}_{SR}\hat{h}_{RD})}{\text{var}(\hat{h}_{SRD})} = 1 \quad (60)$$

indicating that the statistics of two estimates converge to each other and, ultimately, two estimators perform equivalently⁵. Under this assumption, we have $\Psi_{|\hat{h}_{SRD}|^2}(-s) \approx \Psi_{|\hat{h}_{SR}\hat{h}_{RD}|^2}(-s)$ which is given by

$$\begin{aligned} \Psi_{|\hat{h}_{SR}\hat{h}_{RD}|^2}(-s) &= \frac{1}{s\sigma_{\hat{h}_{SR}}^2\sigma_{\hat{h}_{RD}}^2} \exp \left(\frac{1}{s\sigma_{\hat{h}_{SR}}^2\sigma_{\hat{h}_{RD}}^2} \right) \\ &\times \Gamma \left(0, \frac{1}{s\sigma_{\hat{h}_{SR}}^2\sigma_{\hat{h}_{RD}}^2} \right). \end{aligned} \quad (61)$$

Replacing $\Psi_{|\hat{h}_{SD}|^2}$ and $\Psi_{|\hat{h}_{SR}\hat{h}_{RD}|^2}$ in (54), we obtain

$$\begin{aligned} P(\mathbf{x} \rightarrow \hat{\mathbf{x}}) &< \frac{4SNR_{eff}^{-2} / (\lambda_{\min}^2 \kappa_1 \kappa_2)}{(1 - \sigma_{e_{SD}}^2) (1 - \sigma_{e_{SR}}^2) (1 - \sigma_{e_{RD}}^2)} \\ &\times \exp \left(\frac{2SNR_{eff}^{-1} / (\lambda_{\min} \kappa_2)}{(1 - \sigma_{e_{SR}}^2) (1 - \sigma_{e_{RD}}^2)} \right) \\ &\times \Gamma \left(0, \frac{2SNR_{eff}^{-1} / (\lambda_{\min} \kappa_2)}{(1 - \sigma_{e_{SR}}^2) (1 - \sigma_{e_{RD}}^2)} \right) \end{aligned} \quad (62)$$

which yields (26).

⁵Their equivalent performance has been further confirmed through simulated BER performance of mismatched receiver.

$$P(\mathbf{x} \rightarrow \hat{\mathbf{x}} | \hat{\mathbf{h}}) \leq \exp \left(-E \frac{|\alpha|^2 (\bar{\lambda}_1 + \Theta^2 \bar{\lambda}_2) |\hat{h}_{SD}|^2 + |\bar{\alpha}|^2 A_2 (\bar{\lambda}_1 + \bar{\Theta}^2 \bar{\lambda}_2) |\hat{h}_{SD}|^2 + |\alpha|^2 A_1 (\bar{\lambda}_1 + \Theta^2 \bar{\lambda}_2) |\hat{h}_{SRD}|^2}{4\Lambda} \right) \quad (53)$$

$$P(\mathbf{X}_D \rightarrow \hat{\mathbf{X}}_D | \hat{\varphi}, |\mathbf{h}|) = P \left(\|\mathbf{r}\|^2 - 2\text{Re} \{ \mathbf{r}^H (\mathbf{X}_D \hat{\varphi}) \} + \|\mathbf{X}_D \hat{\varphi}\|^2 > \|\mathbf{r}\|^2 - 2\text{Re} \{ \mathbf{r}^H (\hat{\mathbf{X}}_D \hat{\varphi}) \} + \|\hat{\mathbf{X}}_D \hat{\varphi}\|^2 \right) \quad (67)$$

$$\begin{aligned} P(\mathbf{X}_D \rightarrow \hat{\mathbf{X}}_D | \varepsilon, |\mathbf{h}|) &= P(2\text{Re} \{ (|h_{SD}| E e^{-j\varepsilon_{SD}} + |h_{SRD}| B_1 E e^{-j\varepsilon_{SRD}}) x^* (\hat{x} - x) \} + n' > 0) \\ &= P(n' > 2|h_{SD}| E (\cos(\varepsilon_{SD}) - \cos(\varepsilon_{SD} + \theta_\Delta)) + 2|h_{SRD}| B_1 E (\cos(\varepsilon_{SRD}) - \cos(\varepsilon_{SRD} + \theta_\Delta))) \end{aligned} \quad (71)$$

$$= Q \left(\frac{2|h_{SD}| E (\cos(\varepsilon_{SD}) - \cos(\varepsilon_{SD} + \theta_\Delta)) + 2|h_{SRD}| B_1 E (\cos(\varepsilon_{SRD}) - \cos(\varepsilon_{SRD} + \theta_\Delta))}{\sqrt{\text{var}(n')}} \right) \quad (72)$$

APPENDIX B

In this appendix, we present the derivation of PEP for OAF protocol with mismatched-coherent detector. The Chernoff bound on the PEP is given by (46) where \mathbf{X}_D is defined by (17) and the effective noise term $\bar{\mathbf{n}} = \mathbf{n} + \mathbf{X}_D \mathbf{e}$ is assumed to be Gaussian with

$$\begin{aligned} \Lambda &= \text{trace} (E \{ \bar{\mathbf{n}} \bar{\mathbf{n}}^H \}) \\ &= 2N_0 + B_1 \sigma_{e_{SRD}}^2 E + \sigma_{e_{SD}}^2 E. \end{aligned} \quad (63)$$

The unconditional PEP can be found as

$$P(x \rightarrow \hat{x}) \leq \Psi_{|\hat{h}_{SD}|^2} \left(\frac{-E\lambda}{4\Lambda} \right) \Psi_{|\hat{h}_{SRD}|^2} \left(\frac{-B_1 E \lambda}{4\Lambda} \right) \quad (64)$$

where $\lambda = |x - \hat{x}|^2$. $\Psi_{|\hat{h}_{SD}|^2}$ and $\Psi_{|\hat{h}_{SRD}|^2}$ are already given by (55) and (61) respectively. Replacing them in (64), we have

$$\begin{aligned} P(x \rightarrow \hat{x}) &\leq \frac{4SNR_{eff}^{-2} / (\lambda^2 B_1)}{(1 - \sigma_{e_{SD}}^2) (1 - \sigma_{e_{SR}}^2) (1 - \sigma_{e_{RD}}^2)} \\ &\times \exp \left(\frac{2SNR_{eff}^{-1} / (\lambda B_1)}{(1 - \sigma_{e_{SR}}^2) (1 - \sigma_{e_{RD}}^2)} \right) \\ &\times \Gamma \left(0, \frac{2SNR_{eff}^{-1} / (\lambda B_1)}{(1 - \sigma_{e_{SR}}^2) (1 - \sigma_{e_{RD}}^2)} \right) \end{aligned} \quad (65)$$

which yields (32).

APPENDIX C

In this appendix, we present the derivation of PEP for OAF protocol with partially-coherent detector. For this case, PEP is given by

$$\begin{aligned} P(\mathbf{X}_D \rightarrow \hat{\mathbf{X}}_D | \hat{\varphi}, |\mathbf{h}|) &= \\ P \left(\|\mathbf{r} - \mathbf{X}_D \hat{\varphi}\|^2 > \|\mathbf{r} - \hat{\mathbf{X}}_D \hat{\varphi}\|^2 \right) \end{aligned} \quad (66)$$

which can be expanded as (67) (which can be found at the top of this page).

Recall that \mathbf{X}_D and $\hat{\mathbf{X}}_D$ consist of M-PSK modulated transmitted symbols with unit energy⁶. Thus, we have $\|\mathbf{X}_D \hat{\varphi}\|^2 = \|\hat{\mathbf{X}}_D \hat{\varphi}\|^2$ which lets us rewrite (67) as

$$\begin{aligned} P(\mathbf{X}_D \rightarrow \hat{\mathbf{X}}_D | \hat{\varphi}, |\mathbf{h}|) &= P(2\text{Re} \{ \mathbf{r}^H (\hat{\mathbf{X}}_D \hat{\varphi} - \mathbf{X}_D \hat{\varphi}) \} > 0) \end{aligned} \quad (68)$$

$$= P(2\text{Re} \{ \mathbf{h}^H \mathbf{X}_D^H (\hat{\mathbf{X}}_D - \mathbf{X}_D) \hat{\varphi} + \mathbf{n}^H (\hat{\mathbf{X}}_D - \mathbf{X}_D) \hat{\varphi} \} > 0) \quad (69)$$

where (69) is simply obtained from (68) replacing $\mathbf{r} = \mathbf{X}_D \mathbf{h} + \mathbf{n}$. Defining the phase difference between the transmitted symbol and incorrect decision as $\theta_\Delta = \theta_x - \theta_{\hat{x}}$, the variance of the effective noise $n' = 2\text{Re} \{ \mathbf{n}^H (\hat{\mathbf{X}}_D - \mathbf{X}_D) \hat{\varphi} \}$ can be obtained as [31]

$$\begin{aligned} \text{var}(n') &= 2N_0 E (1 + B_1) |\hat{x} - x|^2 \\ &= 4N_0 E (1 - \cos(\theta_\Delta)) (1 + B_1) \end{aligned} \quad (70)$$

where $|\hat{x} - x|^2 = |x|^2 + |\hat{x}|^2 - 2\text{Re} \{ \hat{x}^* x \} = 2(1 - \cos(\theta_\Delta))$. Using $\varepsilon_{SRD} = \varphi_{SRD} - \hat{\varphi}_{SRD}$ and $\varepsilon_{SD} = \varphi_{SD} - \hat{\varphi}_{SD}$, (69) can be rewritten as in (71) and (72) (both of which can be found at the top of this page).

Unconditional PEP can be found by averaging (72) with respect to $|\mathbf{h}|$ and ε . However, this averaging can be much complicated due to cross terms [23]. In order to simplify proceeding derivation steps, we further upper bound (72) as in (73) (which can be found at the top of the next page) ignoring the cross terms resulting from squaring the numerator of the Q function in (72). Under the assumption that phase estimate errors are sufficiently small for high PLL loop gain, the expectation of (73) with respect to ε can be approximated by replacing the terms $\cos(\varepsilon_{SD}) - \cos(\varepsilon_{SD} + \theta_\Delta)$ and $\cos(\varepsilon_{SRD}) - \cos(\varepsilon_{SRD} + \theta_\Delta)$ with their expected values [32], i.e., $\cos(\varepsilon_{SD}) - \cos(\varepsilon_{SD} + \theta_\Delta) \approx (1 - \cos(\theta_\Delta)) E \{ \cos(\varepsilon_{SD}) \} + \sin(\theta_\Delta) E \{ \sin(\varepsilon_{SD}) \}$ where

$$E \{ \sin(\varepsilon_{SD}) \} \cong E \{ \varepsilon_{SD} \} = 1/\rho_{SD}, \quad (74)$$

$$\begin{aligned} E \{ \cos(\varepsilon_{SD}) \} &= \int_{-\pi}^{\pi} \cos(\varepsilon'_{SD}) \frac{e^{\rho_{SD} \cos(\varepsilon'_{SD})}}{2\pi I_0(\rho_{SD})} d\varepsilon'_{SD} \\ &= I_1(\rho_{SD}) / I_0(\rho_{SD}). \end{aligned} \quad (75)$$

⁶Since the amplitude information is essential for QAM signals, the derivation in this Appendix applies only to M-PSK signals.

$$P(x \rightarrow \hat{x} | \varepsilon, |\mathbf{h}|) < Q \left(\sqrt{\frac{|h_{SD}|^2 E (\cos(\varepsilon_{SD}) - \cos(\varepsilon_{SD} + \theta_\Delta))^2 + |h_{SRD}|^2 B_1^2 E (\cos(\varepsilon_{SRD}) - \cos(\varepsilon_{SRD} + \theta_\Delta))^2}{N_0 (1 - \cos(\theta_\Delta)) (1 + B_1)}} \right) \quad (73)$$

$$P(x \rightarrow \hat{x}) < \underbrace{E_{|h_{SD}|^2} \left\{ \exp \left(-\frac{E |h_{SD}|^2 (\Delta_1 - (1 - \cos(\theta_\Delta) - 2 \sin(\theta_\Delta))/2\rho_{SD})^2}{\Omega} \right) \right\}}_{E_1} \times \underbrace{E_{|h_{SR} h_{RD}|^2} \left\{ \exp \left(-\frac{E |h_{SRD}|^2 B_1^2 (\Delta_1 - (1 - \cos(\theta_\Delta) - 2 \sin(\theta_\Delta))/2\rho_{SRD})^2}{\Omega} \right) \right\}}_{E_2} \quad (78)$$

Here, $I_1(\cdot)$ and $I_0(\cdot)$ are the first and zero order modified Bessel functions of the first kind and $\rho_{SD} = |h_{SD}|^2 E / N_0 B_L T$. Similarly, for S→R→D link phase error, we obtain $\cos(\varepsilon_{SRD}) - \cos(\varepsilon_{SRD} + \theta_\Delta) \approx (1 - \cos(\theta_\Delta)) I_1(\rho_{SRD}) / I_0(\rho_{SRD}) + \sin(\theta_\Delta) / \rho_{SRD}$ where $\rho_{SRD} = |h_{SR}|^2 |h_{RD}|^2 B_1 E / N_0 B_L T$. Replacing these approximations in (73) and applying the Chernoff bound, we have,

$$P(x \rightarrow \hat{x} | |\mathbf{h}|) < \exp \left(-\frac{|h_{SD}|^2 E (\Delta_1 I_1(\rho_{SD}) / I_0(\rho_{SD}) + \sin(\theta_\Delta) / \rho_{SD})^2}{\Omega} \right) \times \exp \left(-\frac{|h_{SRD}|^2 B_1^2 E (\Delta_1 I_1(\rho_{SRD}) / I_0(\rho_{SRD}) + \sin(\theta_\Delta) / \rho_{SRD})^2}{\Omega} \right) \quad (76)$$

where $\Delta_1 = 1 - \cos(\theta_\Delta)$ and $\Omega = 2N_0 \Delta_1 (1 + B_1)$. To find the unconditional PEP, we still need to take an expectation with respect to $|\mathbf{h}|$. For high loop SNRs, the ratio of two Bessel functions in (76) can be approximated as [28]

$$I_1(\rho_{SD}) / I_0(\rho_{SD}) \approx 1 - 1/2\rho_{SD}, \quad (77)$$

$$I_1(\rho_{SRD}) / I_0(\rho_{SRD}) \approx 1 - 1/2\rho_{SRD}.$$

Then, (76) simplifies to (78) (which can be found at the top of this page). Noting $|h_{SD}|^2$ is central chi-squared distributed with second degree of freedom, E_1 can be calculated as

$$E_1 = \exp \left(\frac{\Delta_1 \Delta_2}{\Omega / N_0 B_L T} \right) \times \int_0^\infty \exp \left(-\alpha \left(\frac{\Delta_1^2 E}{\Omega} + 1 \right) - \frac{1}{4\alpha} \left(\frac{\Delta_2^2 (N_0 B_L T)^2}{E \Omega} \right) \right) d\alpha \quad (79)$$

where $\Delta_2 = 1 - \cos(\theta_\Delta) - 2 \sin(\theta_\Delta)$. Using the integral result $\int_0^\infty \exp(-\beta/4x - tx) dx = \sqrt{\beta/t} K_1(\sqrt{\beta t})$ [26], (79) yields

$$E_1 = \exp \left(\frac{\Delta_1 \Delta_2}{\Omega / N_0 B_L T} \right) \sqrt{\frac{\Delta_2^2 (N_0 B_L T / E)^2}{\Delta_1^2 + \Omega / E}} \times K_1 \left(\sqrt{\Delta_2^2 \left(\Delta_1^2 \left(\frac{N_0 B_L T}{\Omega} \right)^2 + \frac{(N_0 B_L T)^2}{E \Omega} \right)} \right) \quad (80)$$

where K_1 is the first order modified Bessel function of second kind. Noting $|h_{SR}|^2$ and $|h_{RD}|^2$ are chi-squared distributed, we have E_2 as in (81) (which can be found at the top of the next page). There is, unfortunately, no closed form solution of the integral given in (81). However, using the approximation $K_\nu(z) \approx 0.5\Gamma(\nu) (2/z)^\nu$, $z < 1$ [28] which gives satisfactory results for small $B_L T$ values, we can readily solve (81) as

$$E_2 = \frac{\Omega}{B_1^2 E \Delta_1^2} \exp \left(\frac{B_1 \Delta_1 \Delta_2}{\Omega / N_0 B_L T} + \frac{\Omega}{B_1^2 E \Delta_1^2} \right) \Gamma \left(0, \frac{\Omega}{B_1^2 E \Delta_1^2} \right) \quad (82)$$

Replacing (80) and (82) in (78), we obtain

$$P(x \rightarrow \hat{x}) < \frac{SNR_{eff}^{-2}}{B_1^2 \Delta_1^2} \sqrt{\frac{(\Delta_2 B_L T / (2\Delta_1 + 2B_1 \Delta_1))^2}{\Delta_1^2 + SNR_{eff}^{-1}}} \times \exp \left(\frac{\Delta_2 B_L T}{2} + \frac{SNR_{eff}^{-1}}{B_1^2 \Delta_1^2} \right) \Gamma \left(0, \frac{SNR_{eff}^{-1}}{B_1^2 \Delta_1^2} \right) \times K_1 \left(\sqrt{\left(\frac{\Delta_2 B_L T}{2 + 2B_1} \right)^2 + \frac{(\Delta_2 B_L T / (2 + 2B_1))^2 SNR_{eff}^{-1}}{\Delta_1^2}} \right) \quad (83)$$

REFERENCES

- [1] A. Sendonaris, E. Erkip, and B. Aazhang, "User cooperation diversity part I: system description," *IEEE Trans. Commun.*, vol. 51, no. 11, pp. 1927-1938, Nov. 2003.
- [2] J. N. Laneman and G. W. Wornell, "Distributed space-time-coded protocols for exploiting cooperative diversity in wireless networks," *IEEE Trans. Inform. Theory*, vol. 49, no. 10, pp. 2415-2425, Oct. 2003.
- [3] R. U. Nabar, H. Bölcskei, and F. W. Kneubühler, "Fading relay channels: performance limits and space-time signal design," *IEEE J. Select. Areas Commun.*, vol. 22, no. 6, pp. 1099-1109, Aug. 2004.
- [4] A. Nosratinia, T. E. Hunter, and A. Hedayat, "Cooperative communication in wireless networks," *IEEE Commun. Mag.*, vol. 42, no. 10, pp. 68-73, Oct. 2004.
- [5] V. Stankovic, A. Host-Madsen, and Z. Xiong, "Cooperative diversity for wireless ad-hoc networks," *IEEE Signal Processing Mag.*, vol. 23, pp. 37-49, Sept. 2006.
- [6] A. Scaglione, D. Goeckel, and J. N. Laneman, "Cooperative communications in mobile ad-hoc networks: rethinking the link abstraction," *IEEE Signal Processing Mag.*, vol. 23, no. 5, pp. 18-29, Sept. 2006.
- [7] P. Tarasak, H. Minn, and V. K. Bhargava, "Differential modulation for two-user cooperative diversity systems," *IEEE J. Select. Areas Commun.*, vol. 23, no. 9, pp. 1891-1900, Sept. 2005.
- [8] T. Himsoon, W. Su, and K. J. R. Liu, "Differential transmission for amplify-and-forward cooperative communications," *IEEE Signal Processing Lett.*, vol. 12, no. 9, pp. 597-600, Sept. 2005.
- [9] D. Chen and J. N. Laneman, "Modulation and demodulation for cooperative diversity in wireless systems," *IEEE Trans. Wireless Commun.*, vol. 5, no. 7, pp. 1785-1794, July 2006.
- [10] T. Kiran and B. S. Rajan, "Partially-coherent distributed space-time codes with differential encoder and decoder," *IEEE J. Select. Areas Commun.*, vol. 25, no. 2, pp. 426-433, Feb. 2007.
- [11] H. Mheidat and M. Uysal, "Non-coherent and mismatched-coherent receivers for distributed STBCs with amplify-and-forward relaying," *IEEE Trans. Wireless Commun.*, vol. 6, no. 11, pp. 4060-4070, Nov. 2007.

$$E_2 = \exp\left(\frac{B_1 \Delta_1 \Delta_2}{\Omega / N_0 B_L T}\right) \int_0^\infty \sqrt{\frac{\Delta_2^2 (N_0 B_L T / \alpha_2 B_1 E)^2}{\Delta_1^2 + \Omega / \alpha_2 B_1^2 E}} K_1 \left(\sqrt{\Delta_2^2 B_1^2 \left(\Delta_1^2 \left(\frac{N_0 B_L T}{\Omega} \right)^2 + \frac{(N_0 B_L T)^2}{\alpha_2 B_1^2 E \Omega} \right)} \right) \exp(-\alpha_2) d\alpha_2 \quad (81)$$

- [12] H. Mheidat and M. Uysal, "Impact of receive diversity on the performance of amplify-and-forward relaying under aps and ips power constraints," *IEEE Commun. Lett.*, vol. 10, no. 6, pp. 468-470, June 2006.
- [13] M. Uysal and H. Mheidat, "Maximum-likelihood detection for distributed space-time block coding," in *Proc. IEEE VTC'04-Fall*, Los Angeles, Sept. 2004.
- [14] C. S. Patel, "Wireless channel modeling, simulation and estimation," Ph.D. thesis, Georgia Institute of Technology, May 2006.
- [15] C. S. Patel and G.L. Stuber, "Channel estimation for amplify and forward relay based cooperation diversity systems," *IEEE Trans. Wireless Commun.*, vol. 6, no. 6, pp. 2348-2356, June 2007.
- [16] J. N. Laneman, D. N. C. Tse, and G. W. Wornell, "Cooperative diversity in wireless networks: efficient protocols and outage behavior," *IEEE Trans. Inform. Theory*, vol. 50, no. 12, pp. 3062-3080, Dec. 2004.
- [17] K. Azarian, H. E. Gamal, and P. Schniter, "On the achievable diversity-multiplexing tradeoff in half-duplex cooperative channels," *IEEE Trans. Inform. Theory*, vol. 51, no. 12, pp. 4152-4172, Dec. 2005.
- [18] H. Ochiai, P. Mitran, and V. Tarokh, "Design and analysis of collaborative diversity protocols for wireless sensor networks," in *Proc. VTC Fall*, pp. 4645-4649, Sept. 2004.
- [19] J. C. Belfiore, G. Rekaya, and E. Viterbo, "The golden code: a 2 x 2 full-rate space-time code with non-vanishing determinants," *IEEE Trans. Inform. Theory*, vol. 51, no. 4, Apr. 2005.
- [20] S. Yang and J. C. Belfiore, "Optimal space-time codes for the MIMO amplify-and-forward cooperative channel," *IEEE Trans. Inform. Theory*, vol. 53, no. 2, pp. 647-663, Feb. 2007.
- [21] D. Chen and J. N. Laneman, "Cooperative diversity for wireless fading channels without channel state information," in *Proc. Asilomar Conf. Signals, Systems Computers*, Monterey, CA, Nov. 2004.
- [22] G. Taricco and E. Biglieri, "Space-time decoding with imperfect channel estimation," *IEEE Trans. Wireless Commun.*, vol. 4, no. 4, pp. 1874-1888, July 2005.
- [23] M. K. Simon and M. S. Alouini, *Digital Communications over Fading Channels*. New York: Wiley, 2000.
- [24] S. M. Kay, *Fundamentals of Statistical Signal Processing: Estimation Theory*. Prentice-Hall, 1993.
- [25] A. J. Viterbi, *Principles of Coherent Communication*. New York: McGraw-Hill, 1966.
- [26] I. S. Gradshteyn and I. M. Ryzhik, *Table of Integrals, Series, and Products*. San Diego: Academic Press, 5th ed., 1994.
- [27] R. J. Serfling, *Approximation Theorems of Mathematical Statistics*. New York: Wiley, 1980.
- [28] M. Abramowitz and I. A. Stegun, *Handbook of Mathematical Functions*. New York: Dover Pub., 1964.
- [29] M. M. Fareed and M. Uysal, "BER-optimized power allocation for fading relay channels," *IEEE Trans. Wireless Commun.*, vol. 7, no. 6, pp. 2350-2359, June 2008.
- [30] B. Hassibi and B.M. Hochwald, "How much training is needed in multiple antenna wireless links," *IEEE Trans. Inform. Theory*, vol. 49, no. 4, pp. 951-963, Apr. 2003.
- [31] E. Zehavi and G. Kaplan, "Phase noise effects on M-ary PSK trellis codes," *IEEE Trans. Commun.*, vol. 39, no. 3, pp. 373-379, Mar. 1991.
- [32] T. Eng and L. B. Milstein, "Partially coherent DS-SS performance in frequency selective multipath fading," *IEEE Trans. Wireless Commun.*, vol. 45, no. 1, pp. 110-118, Jan. 1997.
- [33] W. J. Weber, "Performance of phase-locked loops in the presence of fading communication channels," *IEEE Trans. Commun.*, vol. 24, no. 5, pp. 487-499, May 1976.
- [34] M. O. Damen, H. El Gamal, and G. Caire, "On maximum-likelihood detection and the search of the closest lattice point," *IEEE Trans. Inform. Theory*, vol. 49, no. 10, pp. 2389-2402, Oct. 2003.
- [35] B. Hassibi and H. Vikalo, "On the sphere decoding algorithm: part I and II," *IEEE Trans. Signal Processing*, vol. 53, no. 8, pp. 2806-2834, Aug. 2005.
- [36] K. Ahmed, C. Tepedelenioglu, and A. Spanias, "Performance of precoded OFDM with channel estimation error," *IEEE Trans. Signal Processing*, vol. 54, no. 3, pp. 1165-1171, Mar. 2006.
- [37] T. Q. S. Quek, H. Shin, and M. Win, "Robust wireless relay networks: slow power allocation with guaranteed QoS," *IEEE J. Select. Topics Signal Processing*, Dec. 2007.



Berna Gedik was born in Ankara, Turkey in 1982. She received B.Sc. in Electrical and Electronics Engineering from Middle East Technical University (METU), Ankara, Turkey, in 2004 and M.S. in Electrical Engineering from University of Waterloo, Waterloo, Ontario, Canada in 2008. She is currently affiliated with General Electric Company. Her research interests include cooperative communications and wireless channel estimation.



Murat Uysal was born in Istanbul, Turkey in 1973. He received the B.Sc. and the M.Sc. degree in electronics and communication engineering from Istanbul Technical University, Istanbul, Turkey, in 1995 and 1998, respectively, and the Ph.D. degree in electrical engineering from Texas A&M University, College Station, Texas, in 2001. Since 2002, he has been with the Department of Electrical and Computer Engineering, University of Waterloo, Canada, where he is now an Associate Professor. His general research interests lie in communications theory and

signal processing for communications with special emphasis on wireless applications. Specific research areas include space-time coding, MIMO techniques, performance analysis over fading channels, and cooperative communications.

Dr. Uysal is an Associate Editor for IEEE TRANSACTIONS ON WIRELESS COMMUNICATIONS and IEEE COMMUNICATIONS LETTERS. He also served as a Guest Co-Editor for Wiley JOURNAL ON WIRELESS COMMUNICATIONS AND MOBILE COMPUTING's Special Issue on "MIMO Communications" published in 2004. Over the years, he has served on the technical program committee of more than 50 international conferences in the communications area. He recently co-chaired IEEE ICC'07 Communication Theory Symposium and chaired CCECE'08 Communications and Networking Symposium. Dr. Uysal is a Senior IEEE member.